

## Structural, morphological, optical and electrochemical characterization of Ag<sub>2</sub>O/ZnO and ZnO/Ag<sub>2</sub>O nanocomposites

W. H. Al-Qahtani<sup>a</sup>, G. Murugadoss<sup>b,\*</sup>, K. Narthana<sup>b</sup>, M. R. Kumar<sup>c</sup>,  
J. R. Rajabathar<sup>d</sup>, A. Kathalingam<sup>e</sup>

<sup>b</sup>Centre for Nanoscience and Nanotechnology, Sathyabama Institute of Science and Technology, Chennai 600119, Tamil Nadu, India

<sup>c</sup>Institute of Natural Science and Mathematics, Ural Federal University, Yekaterinburg 620002, Russia

<sup>a</sup>Department of Food Sciences & Nutrition, College of Food & Agriculture Sciences, King Saud University, Riyadh 11451, Saudi Arabia

<sup>d</sup>Chemistry Department, College of Science, King Saud University, P.O. Box. 2455, Riyadh 11451, Kingdom of Saudi Arabia.

<sup>e</sup>Millimeter-wave Innovation Technology Research Center, Dongguk University, Seoul 04620, South Korea

In this paper, well-crystalline Ag<sub>2</sub>O/ZnO and ZnO/Ag<sub>2</sub>O nanocomposites were prepared by a facile chemical method. Structural, morphological and optical properties of the nanocomposite were studied using various advanced characterization techniques such as X-ray diffraction (XRD), scanning electron microscopy (SEM), transmission electron microscopy (TEM), Fourier-transform infrared spectroscopy (FTIR), UV-Visible (UV-Vis) and photoluminescence (PL) spectroscopy. The Ag<sub>2</sub>O and ZnO were clearly identified in the composite from SEM and TEM. Significant shifting observed in the both UV-Vis and PL spectroscopy. In addition, electrocatalytic activity of the Ag<sub>2</sub>O/ZnO and ZnO/Ag<sub>2</sub>O nanocomposites studied by an electrochemical workstation. The ZnO/Ag<sub>2</sub>O nanocomposites showed better optical and electrochemical properties due to decorating the low-band gap Ag<sub>2</sub>O on the surface of hexagonal structure ZnO nanoparticles.

(Received December 14, 2021; Accepted March 22, 2022)

**Keywords:** Nanocomposite, Heterostructure, Blue shift, Photoluminescence, Electrochemistry

### 1. Introduction

Semiconductor nanomaterials are the most widely studied types of energy production consents [1,2]. Silver nanoparticles are one of the widely used materials in the world production in the range of 360–450 tons per year. Silver particles have multifunctional properties that are the reason it is very demand in producers' side. It is now well established that Ag nanoparticles have antimicrobial, antifungal, antiviral, catalytic, sensory and other properties which make it possible to apply them in various field: water treatment, textile manufacture, chemical industry, medicine, pharmaceutical industry, etc. There are currently a number of traditional methods know to produce silver nanoparticles with specific physiochemical properties, such as physical, chemical, photochemical and biological methods. Zinc oxide (ZnO) is another interesting material, mainly it can be used as a photocatalyst and has drawn more attention due to its attractive photocatalytic performance [3,4]. The photocatalytic activity of metal oxide nanoparticles is closely associated with the surface morphology [5]. The ZnO nanoparticles with hierarchical and hexagonal-like morphology demonstrated attracting application in degradation of textile dyes due to the increased optical absorption efficiency and high specific surface area [6,7]. However, because of the wide

---

\* Corresponding author: murugadoss\_g@yahoo.com  
<https://doi.org/10.15251/JOR.2022.182.187>

band gap of ZnO (3.2 eV), only limited range of solar radiation can be used and the photogenerated charge carriers are liable to recombination, leading to low quantum yields. In order to improve its photocatalytic performance, one of approach is to combine ZnO with a narrow-band material with cover a wider range of light absorption and a minimum rate of the recombination of photogenerated charge carriers.

For the past few decades, several reports focused on the higher photocatalytic efficiency of ZnO by coupling with appropriate nanomaterials such as TiO<sub>2</sub>, Bi<sub>2</sub>O<sub>3</sub>, CuO and ZnS [8–11]. The efficiency enhancement on the degradation of textile dye can be ascribed to the effective separation of photoinduced charge carriers. Moreover, the charge carrier separation would be significantly improved and highly efficient particularly in the inner electric field, which was formed by a p-n-type, such as CuO/ZnO [12] and NiO/ZnO [13]. Silver oxide (Ag<sub>2</sub>O) is an interesting p-type semiconductor with a low band gap (1.3 eV). Recently, TiO<sub>2</sub> and Bi<sub>2</sub>O<sub>3</sub> were effectively modified using silver oxide by decorated on the bare metal oxide surface [14]. According to the heterojunction of Ag<sub>2</sub>O and TiO<sub>2</sub>, the recombination of charge carriers was significantly inhibited by moving for the energy band matching and the build-up inner electric field, resulting increase photocatalytic performance [15,16]. To the best of our knowledge, there is no report in the literature on the photocatalytic study together for Ag<sub>2</sub>O/ZnO and reversed ZnO/Ag<sub>2</sub>O nanocomposite.

In this work, mixed crystal structures of Ag<sub>2</sub>O/ZnO and ZnO/Ag<sub>2</sub>O nanocomposites were prepared through a facile chemical method. The as-prepared nanoparticles of Ag<sub>2</sub>O/ZnO and ZnO/Ag<sub>2</sub>O nanocomposites demonstrated good quality of crystalline nature and optical property.

## 2. Experimental details

### 2.1. Materials

Silver (III) nitrate (Ag(NO<sub>3</sub>)<sub>3</sub>, 99%), Zinc acetate (Zn(CH<sub>3</sub>COO)<sub>2</sub>·2H<sub>2</sub>O, 99%), polyvinylpyrrolidone (PVP, MW ~40,000), sodium hydroxide (NaOH, 99%), acetone (CH<sub>3</sub>COCH<sub>3</sub>), ethanol (C<sub>2</sub>H<sub>5</sub>OH, 99.5%), were purchased from Sigma-Aldrich.

### 2.2. Synthesis of Ag<sub>2</sub>O/ZnO and ZnO/Ag<sub>2</sub>O nanocomposite

The Ag<sub>2</sub>O/ZnO and ZnO/Ag<sub>2</sub>O nanocomposite were synthesized by simple chemical precipitation method. Briefly, 0.2 M of Ag(NO<sub>3</sub>)<sub>3</sub> was dissolved in 50 mL of de-ionized water under stirring at 80°C. Then, 1 g of PVP solid powder was added into the above solution. The PVP was used as surfactant to control particle size during the preparation. After 10 min, 2 M of NaOH in 50 mL was added drop wise into the above solution and continued the stirring for 1 h. Then, 0.5 M of (Zn(CH<sub>3</sub>COO)<sub>2</sub>·2H<sub>2</sub>O solution in 50mL ethanol was added drop wise into the above solution under vigorous stirring at room temperature. The resulting mixture was stirred continuously for 2 h. Then, the resultant products were collected by centrifugation, washed with distilled water, ethanol and acetone by several times to remove the impurities and dried the wet sample in hot air oven at 120°C for 2 h. Finally, the powder was collected for characterization. Following the same synthesis procedure, ZnO/Ag<sub>2</sub>O nanocomposite was synthesized by exchanged the chemical of silver nitrate and zinc acetate.

### 2.3. Characterization

The X-ray diffraction (XRD) patterns of the powdered samples were measured using an X'PERTPRO Advance Powder X-ray diffractometer. The morphology of the nanocomposites was investigated using a TEM (Technai20G2, FEI) microscopy. Optical absorption spectra of samples were recorded using a UV-1650PCSHIMADZU spectrometer. Fluorescence study was performed on an RF-5301PC spectrophotometer.

### 2.4. Electrochemical measurements

Electrochemical measurements were performed using Biologic Electrochemical workstation. Three-electrode cell system used for study the electrochemical activity of the nanocomposites. The Ag<sub>2</sub>O/ZnO and ZnO/Ag<sub>2</sub>O were used as a working electrode, a platinum

wire as counter electrode, and Ag/AgCl used as a reference electrode. The Ag<sub>2</sub>O/ZnO and ZnO/Ag<sub>2</sub>O based modified electrodes were fabricated by coating slurry containing a mixture of the nanocomposite (80 wt%), Nafions 117 solution (20 wt%). Then, the coated mesh was dried at 80°C in vacuum for 12 h. The cyclic voltammetry (CV) measurements of the modified electrode were carried out at a scan rate of 20 mV s<sup>-1</sup>.

### 3. Results and discussion

X-ray diffraction (XRD) was used to study the structural information of nanocomposites as shown in Fig. 1(a). In the case of ZnO, the strong diffraction peaks at  $2\theta = 31.7^\circ, 34.4^\circ, 36.3^\circ, 47.5^\circ, 56.6^\circ, 62.9^\circ, 67.9^\circ, 69.1^\circ, 72.5^\circ, 76.9^\circ$  could be assigned as (1 0 0), (0 0 2), (1 0 1), (1 0 2), (1 1 0), (1 0 3), (1 1 2), (2 0 1), (0 0 4) and (2 0 2) (JCPDS card NO. 76-0704), respectively [17]. The diffraction peaks marked with (\*) at  $2\theta = 66.3$  could be indexed to Ag<sub>2</sub>O (2 0 0) respectively, corresponding to cubic structure Ag<sub>2</sub>O (JCPDS card No. 75-1532) [18]. The XRD results are clearly shows that the nanocomposite is composed by the ZnO and Ag<sub>2</sub>O with a high degree of crystallinity. Since the diffraction peaks of ZnO are very strong, the low intensity diffraction peaks of Ag<sub>2</sub>O disappeared. The magnified diffraction peaks of Ag<sub>2</sub>O/ZnO and ZnO/Ag<sub>2</sub>O nanocomposites are shown in Fig. 1(b and c), respectively. The diffraction peaks of Ag<sub>2</sub>O marked with (\*), all the peaks are related to cubic structure Ag<sub>2</sub>O (JCPDS card No. 75-1532) [18].

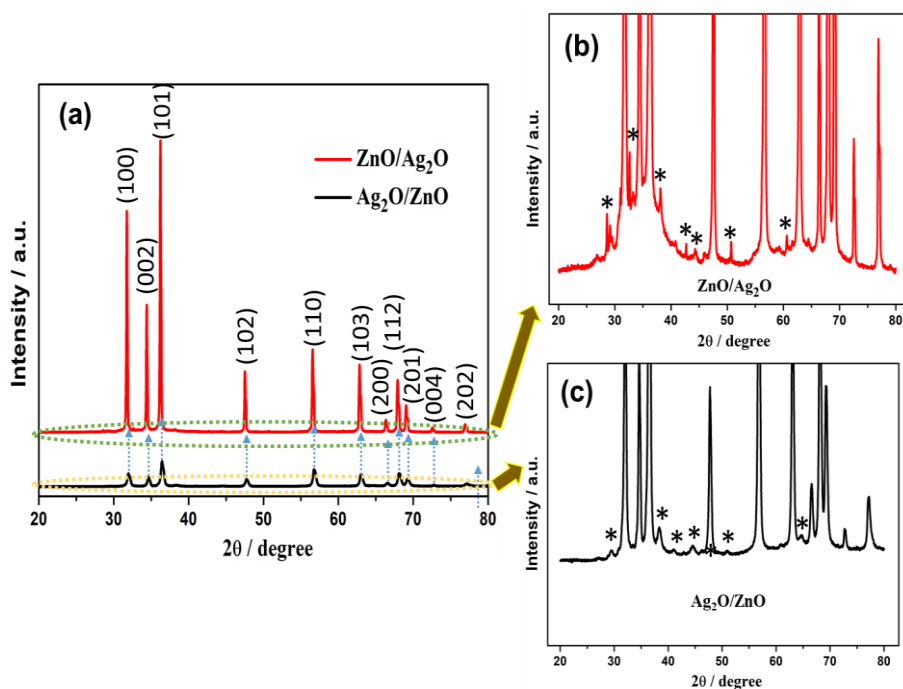


Fig. 1. (a) XRD pattern of the Ag<sub>2</sub>O/ZnO and ZnO/Ag<sub>2</sub>O nanocomposites, (b) Magnified XRD pattern of the ZnO/Ag<sub>2</sub>O and (c) Magnified XRD pattern of the Ag<sub>2</sub>O/ZnO nanocomposites.

In order to obtain the detailed information about the morphology of the nanocomposites, SEM study was carried out, the obtained results are presented in Fig. 2. The Fig. 2(a-b) shows the SEM image of Ag<sub>2</sub>O/ZnO with aggregation of tiny and spherical nanoparticles. The SEM images of ZnO/Ag<sub>2</sub>O nanocomposite showed highly-ordered nanocomposite with decorated or distributed of very tiny Ag<sub>2</sub>O nanoparticles on hexagonal structure of ZnO surface as shown in Fig. 2(c-d). The images showed that ZnO nanoparticles with a diameter of about 100 nm were slightly agglomerated after Ag<sub>2</sub>O impregnated ZnO nanoparticles with a quite uniform shape and size [19]. The SEM observation is clearly showed that the preparation method, particularly the inclusion of precursor time is played a major role to control the morphology of the nanocomposite.

Fig. 3(a-b) and 3(c-d) shows the TEM images with various magnifications of  $\text{Ag}_2\text{O}/\text{ZnO}$  and  $\text{ZnO}/\text{Ag}_2\text{O}$  nanocomposite, respectively. Transmission electron microscopy (TEM) images are clearly showed that the synthesized nanoparticles were spherical and hexagonal structure in shape with an average size of 20 nm and 150 nm, respectively [20]. The corresponding selected area electron diffraction (SAED) pattern exhibited a polycrystalline ZnO hexagonal crystal formation, as shown in Fig. 3a and Fig. 3d, inset. The multiple diffraction rings confirm the mixed phase of the above samples.

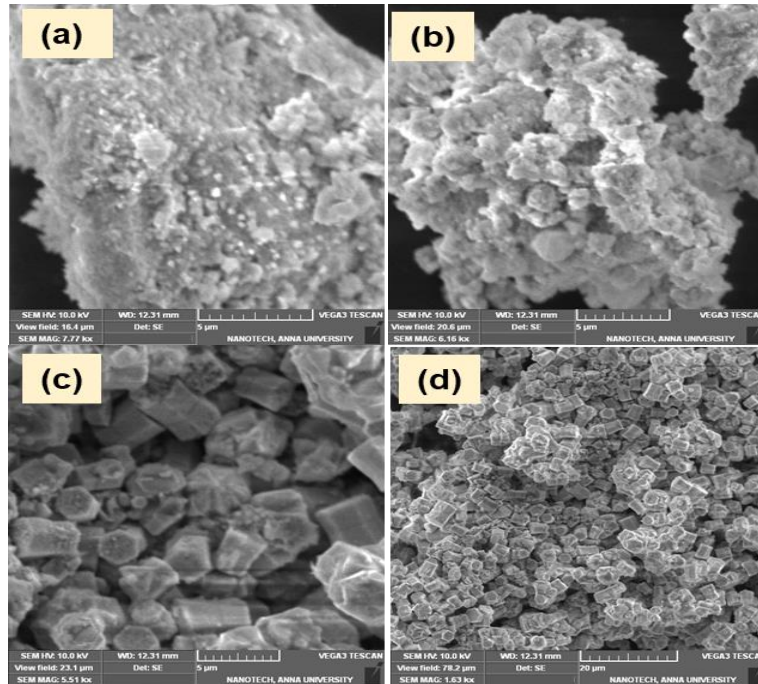


Fig. 2. (a-b) SEM images of the different magnification of  $\text{Ag}_2\text{O}/\text{ZnO}$  and (c-d)  $\text{ZnO}/\text{Ag}_2\text{O}$  nanocomposites.

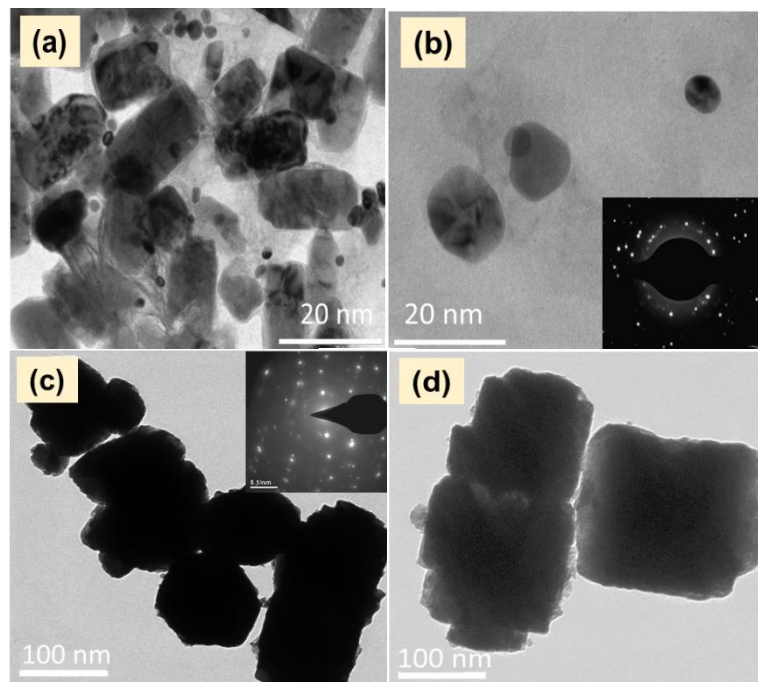


Fig. 3 (a-b) TEM images of the different magnification of  $\text{Ag}_2\text{O}/\text{ZnO}$  and (c-d)  $\text{ZnO}/\text{Ag}_2\text{O}$  nanocomposites.

The FT-IR result of the nanocomposites is showed in Fig. 4. Several well-defined peaks could be observed in the spectrum. The bands obtained at  $588.29\text{ cm}^{-1}$  and  $706\text{ cm}^{-1}$  which is attributed to the Ag-O stretching vibration [21]. The peak located at  $883\text{ cm}^{-1}$  could be assigned to Zn-O bending vibration. The broad peaks at  $3433\text{ cm}^{-1}$  and  $1661\text{ cm}^{-1}$  are ascribed to the stretching and bending vibration of O-H of the adsorbed water molecules on the surface, respectively. The strong bands at  $2918.3\text{ cm}^{-1}$  and  $2882.72\text{ cm}^{-1}$  are representatives of alkaline C-H stretch. Affiant band at  $1647.21\text{ cm}^{-1}$  is a representative of C-H stretch. A band at  $1489.76\text{ cm}^{-1}$  is related to aromatic C-C stretch. Strong bands at  $1382.96\text{ cm}^{-1}$ ,  $1230.58\text{ cm}^{-1}$  and  $1105.21\text{ cm}^{-1}$  are corresponding to C-O stretching vibrations. The additional bands at  $970.19\text{ cm}^{-1}$ ,  $850.61\text{ cm}^{-1}$ ,  $721.38\text{ cm}^{-1}$  and  $626.87\text{ cm}^{-1}$  are due to aromatic C-H bending mode [22].

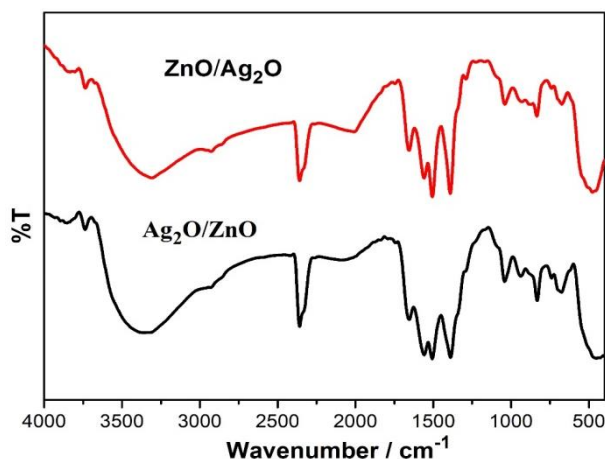


Fig. 4. FTIR spectra of the  $\text{Ag}_2\text{O}/\text{ZnO}$  and  $\text{ZnO}/\text{Ag}_2\text{O}$  nanocomposites.

The optical properties of synthesized samples were probed using UV-vis absorption spectroscopy and displayed the results in Fig. 5a. As estimated, the typical spectrum of  $\text{Ag}_2\text{O}/\text{ZnO}$  and  $\text{ZnO}/\text{Ag}_2\text{O}$  with its fundamental absorption edge arising in the range of 350-400 nm. It is notable that compared to ZnO, the absorption edge slighted towards red region, which may be caused by the  $\text{Ag}_2\text{O}$  in composite. The bulk band gap as  $\text{Ag}_2\text{O}$  has a narrower band gap (2.84 eV) than ZnO (3.37 eV). The absorption intensity of ZnO is stronger than others in the visible region, suggesting an optimal electric surface charge of the oxide within the samples due to the introduction of the  $\text{Ag}_2\text{O}$  which can possibly cause modifications of the fundamental process of electron-hole pair formation during irradiation [23,24].

Room-temperature photoluminescence (PL) measurements is used to characterize the optical properties of nanoparticles. The emission spectra of the  $\text{Ag}_2\text{O}/\text{ZnO}$  and  $\text{ZnO}/\text{Ag}_2\text{O}$  nanocomposites are showed at 525 nm and 750 nm (Fig. 5c-d), respectively. The PL of  $\text{Ag}_2\text{O}/\text{ZnO}$  exist two emission bands: a near band edge emission appeared in the UV range and a visible emission band due to the defects [25]. The two emission peaks for  $\text{Ag}_2\text{O}/\text{ZnO}$  are centred at 525 and 574 nm. In the PL spectrum of  $\text{ZnO}/\text{Ag}_2\text{O}$ , a narrow emission centred at 750 nm. The results were clearly demonstrated that the  $\text{Ag}_2\text{O}$  particles block both direct and trap-related charge carrier recombination pathways since  $\text{Ag}_2\text{O}$  on the ZnO surface can extract electrons from the conduction band of ZnO and act as a sink which can store and shuttle photogenerated electrons.

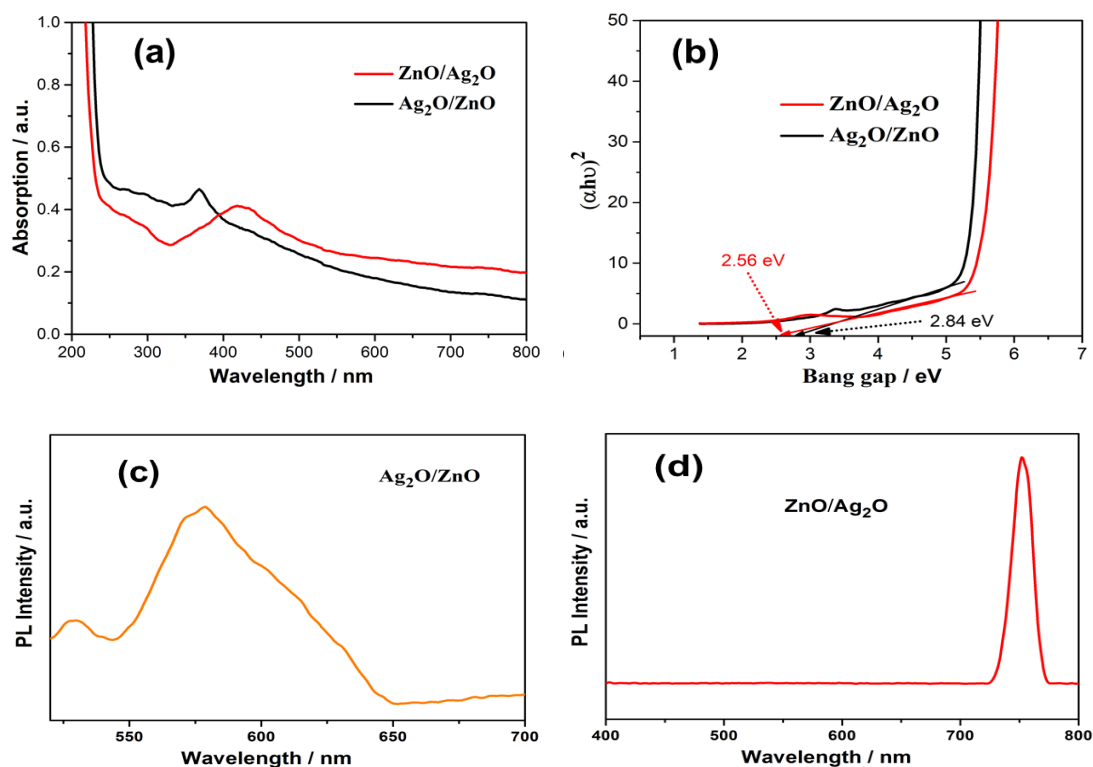


Fig. 5 UV-Visible absorption spectra images of the (a) ZnO/Ag<sub>2</sub>O and Ag<sub>2</sub>O/ZnO, (b) Tauc plot of ZnO/Ag<sub>2</sub>O, Ag<sub>2</sub>O/ZnO nanocomposites, Photoluminescence spectrum of the (c) Ag<sub>2</sub>O/ZnO and (d) ZnO/Ag<sub>2</sub>O nanocomposites, respectively.

To testing electrochemical activity of the Ag<sub>2</sub>O/ZnO and ZnO/Ag<sub>2</sub>O nanocomposites, cyclic voltametric (CV) study was performed. The Fig. 6 shows the CV curves of as-prepared Ag<sub>2</sub>O/ZnO and ZnO/Ag<sub>2</sub>O electrode were analyzed in 0.1 M LiClO<sub>4</sub> in acetonitrile (ACN) electrolyte at constant scan rate of 20 mV/s. The observed potential ranges are different for each sample and it selected based on the materials performance. The selected potential window for Ag<sub>2</sub>O/ZnO is -2.5 to 2V and ZnO/Ag<sub>2</sub>O is -1.2 to 1.14 V, respectively. The CV curves for Ag<sub>2</sub>O/ZnO sample showed one anodic peak in forward scan and straight line occurred at cathodic peak. The ZnO/Ag<sub>2</sub>O showed anodic and cathodic peaks in both forward and backward scan rate [26]. The shape of the CV curves and positions of the oxidation and reduction peaks are changed significantly compared to Ag<sub>2</sub>O/ZnO. The rate of charge transfer depends on the diffusion of anions and cations towards the oxide/solution interface as well as the overlap of the electronic levels in the solid with the redox species in the solution [27]. The peaks shapes indicate that the nanocomposites can be used for supercapacitor and batteries.

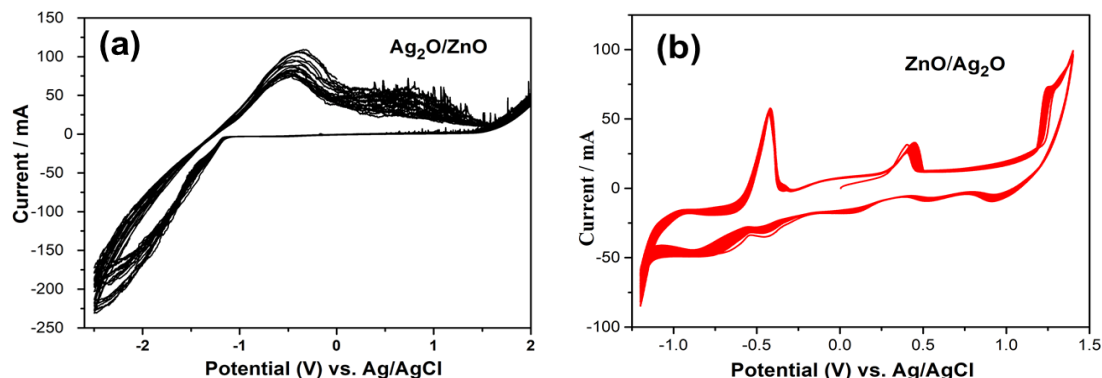


Fig. 6 CV curves of the (a)  $\text{Ag}_2\text{O}/\text{ZnO}$  and (b)  $\text{ZnO}/\text{Ag}_2\text{O}$  nanocomposites.

#### 4. Conclusions

In summary, high quality  $\text{Ag}_2\text{O}/\text{ZnO}$  and  $\text{ZnO}/\text{Ag}_2\text{O}$  nanocomposites were synthesized and characterized using different characterization techniques. Two distinct morphologies obtained for  $\text{Ag}_2\text{O}/\text{ZnO}$  and  $\text{ZnO}/\text{Ag}_2\text{O}$  nanocomposites, additionally, the compounds presence in the nanocomposites were also distinguished. The wider band gap of the ZnO was remarkably reduced by using the low band gap of the  $\text{Ag}_2\text{O}$ . The PL emission is clearly showed in two different regions for the nanocomposites. Interestingly, remarkable oxidation and reduction peaks observed for the  $\text{ZnO}/\text{Ag}_2\text{O}$  nanocomposites with the potential range of -1.2 to 1.14 V. The high potential difference electrode material can be used for supercapacitor and battery application in future.

#### Acknowledgements

Dr. G. Murugadoss would like to acknowledge to the management of Sathyabama Institute of Science and Technology, Chennai, Tamilnadu, India for provided lap facilities. The author (Wahidah H. Al-Qahtani) thank and This work was funded by the Researchers Supporting Project Number (**RSP-2021/293**) King Saud University, Riyadh, Saudi Arabia. One of author (Manavalan Rajesh Kumar) thanks to the contract no. 40/is2.

#### References

- [1] S. Zhao, Y. Zhang, Y. Zhou, C. Zhang, J. Fang, X. Sheng, Appl. Surf. Sci. 410, 344 (2017) <https://doi.org/10.1016/j.apsusc.2017.03.051>
- [2] R. Lamba, A. Umar, S.K. Mehta, S.K. Kansal, Separ. and Purif. Tech. 183, 341 (2017) <https://doi.org/10.1016/j.seppur.2017.03.070>
- [3] D. Khim, Y.H. Lin, S. Nam, H. Faber, K. Tetzner, R. Li, Q. Zhang, J. Li, X. Zhang, T.D. Anthopoulos, Adv. Mater. 29, 1605837 (2017). <https://doi.org/10.1002/adma.201605837>
- [4] R. Zhang, J. Xie, C. Wang, J. Liu, X. Zheng, Y. Li, X. Yang, H.-E. Wang, B.-L. Su, J. Mater. Sci. 52, 11124 (2017). <https://doi.org/10.1007/s10853-017-1130-6>
- [5] Q. Li, P. Wang, S. Liu, Y. Fei, Y. Deng, Green Chem. 18, 6091 (2016) <https://doi.org/10.1039/C6GC01884J>
- [6] N. Venkatesh, S. Aravindan, K. Ramki, G. Murugadoss, R. Thangamuthu, P. Sakthivel, Environ. Sci. and Poll. Res. 28, 16792 (2021). <https://doi.org/10.1007/s11356-020-11763-3>
- [7] M. Zhou, B. Wu, X. Zhang, S. Cao, P. Ma, K. Wang, Z. Fan, M. Su, ACS Appl. Mater. & Interf. 12, 38490 (2020). <https://doi.org/10.1021/acsami.0c03550>

- [8] G. Manibalan, M.R. Kumar, G. Murugadoss, J. Yesuraj, R.M. Kumar, R. Jayavel, *J. Mater. Sci.: Mater. Electron.* 32, 8746 (2021)  
<https://doi.org/10.1007/s10854-021-05546-w>
- [9] N. Foghahazade, M. Mousavi, H. Behnejad, M. Hamzehloo, A. Habibi-Yangjeh, *J. Mater. Sci.: Mater. Electron.* 32, 2704 (2021). <https://doi.org/10.1007/s10854-020-04978-0>
- [10] S. Iqbal, M. Javed, A. Bahadur, M.A. Qamar, M. Ahmad, M. Shoaib, M. Raheel, N. Ahmad, M.B. Akbar, H. Li, *J. Mater. Sci.: Mater. Electron.* 31, 8423 (2020).  
<https://doi.org/10.1007/s10854-020-03377-9>
- [11] W. Hu, Q. Zhang, K. Luo, H. Yuan, J. Li, M. Xu, S. Xu, *Ceramics Inter.* 46, 24753 (2021)  
<https://doi.org/10.1016/j.ceramint.2020.06.235>
- [12] A.O. Juma, E.A. Arbab, C.M. Muiva, L.M. Lepodise, G.T. Mola, *J. Alloys and Compds.* 723, 866 (2017). <https://doi.org/10.1016/j.jallcom.2017.06.288>
- [13] A. Kadam, R. Dhabbe, A. Gophane, T. Sathe, K. Garadkar, *J. Photochem. and Photobio. B: Bio.* 154, 24 (2016). <https://doi.org/10.1016/j.jphotobiol.2015.11.007>
- [14] K. Bhuvaneshwari, G. Palanisamy, G. Bharathi, T. Pazhanivel, I.R. Upadhyaya, M.A. Kumari, R.P. Rajesh, M. Govindasamy, A. Ghfar, N.H. Al-Shaalan, *Environ. Res.* 197, 111079 (2021).  
<https://doi.org/10.1016/j.envres.2021.111079>
- [15] K. Narthana, G. Ramalingam, G. Murugadoss, M.R. Kumar, G. Manibalan, R. Jothi Ramalingam, H.M. Yadav, *J. Alloys and Compds.* 888, 161489 (2021)  
<https://doi.org/10.1016/j.jallcom.2021.161489>
- [16] A. Padmanaban, G. Murugadoss, N. Venkatesh, S. Hazra, M.R. Kumar, R. Tamilselvi, P. Sakthivel, *J. Environ. Chem. Eng.* 9, 105976 (2021). <https://doi.org/10.1016/j.jece.2021.105976>
- [17] M.R. Kumar, G. Murugadoss, N. Venkatesh, P. Sakthivel, *ChemistrySelect* 5, 6946 (2020)  
<https://doi.org/10.1002/slct.202001227>
- [18] M.I. Skiba, V.I. Vorobyova, A. Pivovarov, N.P. Makarshenko, *J. Nanomater.* (2020).  
<https://doi.org/10.1155/2020/3051308>
- [19] Y. Liu, H. Liu, Q. Zhang, T. Li, *RSC Adv.* 7, 3515 (2017).  
<https://doi.org/10.1039/C6RA24912D>
- [20] G. Fan, B. Du, J. Zhou, Z. Yan, Y. You, J. Luo, *Chem. Eng. J.* 404, 126509 (2021)  
<https://doi.org/10.1016/j.cej.2020.126509>
- [21] R.M. Mohamed, A.A. Ismail, M.W. Kadi, A.S. Alresheedi, I.A. Mkhaldid, *ACS Omega* 5, 33269 (2020). <https://doi.org/10.1021/acsomega.0c04969>
- [22] Y. Liu, P. Li, R. Xue, X. Fan, *Chem. Phys. Lett.* 746, 137301 (2020).  
<https://doi.org/10.1016/j.cplett.2020.137301>
- [23] P.L. Meena, K. Poswal, A.K. Surela, J.K. Saini, *Water Sci. and Tech.* 84, 2615 (2021).  
<https://doi.org/10.2166/wst.2021.431>
- [24] M. Rahamim, H. Cohen, E. Edri, *ACS Appl. Mater. & Interf.* 13, 49423 (2021)  
<https://doi.org/10.1021/acsmami.1c11566>
- [25] M.M. Alam, A.M. Asiri, M.M. Rahman, *Microchem. J.* 165, 106092 (2021)  
<https://doi.org/10.1016/j.microc.2021.106092>
- [26] G. Murugadoss, R. Jayavel, R. Thangamuthu, M.R. Kumar, *J. Lumin.* 170, 78 (2016)  
<https://doi.org/10.1016/j.jlumin.2015.10.034>